Available online at www.sciencedirect.com

ScienceDirect

journal homepage: www.elsevier.com/locate/he

Influence of synthesis conditions on the performance of chitosan–Heteropolyacid complexes as membranes for low temperature H_2–O_2 fuel cell

C.M. Pecoraro [a], M. Santamaria [a,*], P. Bocchetta [b], F. Di Quarto [a]

[a] Electrochemical Material Science Laboratory, DICAM, Università di Palermo, Viale delle Scienze, Ed.6, 90128 Palermo, Italy

[b] Dipartimento di Ingegneria dell'Innovazione, Università del Salento, Via Monteroni, 73100 Lecce, Italy

ARTICLE INFO

Article history:
Received 25 February 2015
Received in revised form
8 June 2015
Accepted 16 June 2015
Available online 10 July 2015

Keywords:
Chitosan
Heteropolyacid
Composite membrane
Protonconducting
H_2–O_2 PEMCF

ABSTRACT

Flat, free-standing chitosan/phosphotungstic acid (PTA) polyelectrolyte membranes were prepared by in-situ ionotropic gelation process at room temperature on porous alumina support firstly impregnated by $H_3PW_{12}O_{40}$. Scanning electron microscopy revealed the formation of compact and homogeneous membranes, whose thickness resulted to be dependent on chitosan concentration and reticulation time. X-ray diffraction and Fourier transform infrared spectroscopy (FTIR) evidenced the formation of almost amorphous membrane without appreciable concentration of not protonated NH_2 groups and PTA^{3-} ions with preserved Keggin structure. Membranes were tested as proton conductor in low temperature H_2–O_2 fuel cell allowing to get peak power densities up to 300 mW cm^{-2}. Electrochemical impedance measurements allowed to estimate polyelectrolytes' conductivity up to 28 mS cm^{-1} at room temperature.

Introduction

Proton exchange membrane fuel cells (PEMFCs) have received much attention in recent years because of their high power density [1], efficiency [2], and zero-environmental pollution [3]. As one of the key components in fuel cells, the proton exchange membrane is expected to have high proton conductivity and good electrochemical stability. In the attempt to promote PEMCFs commercialization, high cost of fuel cell systems and short lifecycle are the two main issues that need to be addressed, thus large research effort has been devoted in developing new polymer electrolytes that can replace the usually employed proton conductors, i.e. Nafion®, with other membranes of comparable performances but lower cost.

Perfluorinated ionomers such as Nafion, with fluoroalkyl ether side chains and sulfonic acid end groups on polytetrafluoroethylene backbones, have been the most commonly used polymer electrolyte membrane so far. Nafion material is also used as electrode binder, which facilitates ionic conduction, provides mechanical support for catalyst particles, and enhances dispersion of catalyst particles in the catalyst layer. Nafion possesses many desirable properties as a polymer electrolyte, and yet it is very expensive and loses ionic

* *Corresponding author*. Tel.: +39 09123863787.
E-mail address: monica.santamaria@unipa.it (M. Santamaria).

http://dx.doi.org/10.1016/j.ijhydene.2015.06.083

conductivity if not sufficiently hydrated. As a low-cost and eco-friendly biopolymer, Chitosan (CS)-based membrane electrolyte is currently studied as alternative candidate for PEMFC application to possibly produce economically viable fuel cells.

As cationic polyelectrolyte, CS can react with various natural and synthetic anionic species or anionic polyelectrolytes to form polyelectrolyte complexes (PECs). These complexes are generally water insoluble and make hydrogel. The gelation process is related to the formation of intramolecular hydrophobic interactions between chitosan polymer chains, hydrogen bonding between hydroxyl and amino groups of CS and/or intermolecular bonding with the polyanion counterparts [4,5].

Heteropolyacids (HPAs) are strong Bronsted acid as well as solid electrolytes [6] and are considered promising materials in the fabrication of organic–inorganic nanocomposite membranes for fuel cell thanks to their high proton conductivity [7–10]. The major problems in using HPAs in fuel cell are their solubility in water and low mechanical strength, which might result in decline in cell performance with time [11–15]. To overcome this problem, it has been proposed to prepare CS and HPAs polyelectrolyte films to be employed as proton exchange membrane in low temperature fuel cell, since they are reported to be insoluble [6].

A survey of the already published works on the use of CS/HPA composite membranes show that they have been tested as proton conductors in direct methanol [7–10,16,17], in borohydride [18] and hydrogen [19,20] fed fuel cells. In the last case promising performances were obtained when membranes are prepared on the surface of phosphotungstic acid (PTA) impregnated porous anodic alumina [20].

In this paper we report the results of a physico–chemical characterization of CS/PTA membranes prepared according to such procedure as a function of the fabrication conditions. X-ray diffraction and FTIR analyses were performed to study the structure and composition of the membranes, while Scanning Electron Microscopy was used to get information on the membranes morphology and thickness. The membranes were tested in a H_2/O_2 fuel cell working at low temperature (25 °C) and fixed Pt loading (1 mg cm^{-2}). Impedance Spectroscopy was used to get information of the conductivity of the membrane as well as to model the overall electrical behaviour of the cell.

Experimental

Chitosan/PTA films were grown through ionotropic gelation by using commercial AAM (Anodisc-47 Whatman, pore diameters 200 nm, porosity 43% and thickness 50 μm) as support. Chitosan powder, acetic acid and PTA were supplied by Sigma–Aldrich. The reagents were used as received.

CS powder, distilled water and acetic acid (2% w/v) were mixed to achieve protonation and thus, solubilization of the CS polymer. Solutions were then stirred for 24 h before use. Final chitosan concentrations were equal to 1, 1.5, 2, 2.5 and 3% w/v.

The CS solution was put in contact with an aqueous PTA solution (0.38 M in this work) through a single interface [20] by using the dip-coating procedure according to which a thin film of PTA liquid is entrained by viscous drag on AAM substrate, and afterwards the cross-linking reaction occurs after immersion in the CS aqueous solution the time necessary the reticulation, between 5 s and 60 min in this work.

Once the free-standing CS/PTA thin film was formed and peeled off from AAM support, it was dried for 1 h under atmospheric conditions and then humidified through immersion in pure water for 5 min. The membranes were finally kept immersed in 0.38 M PTA aqueous solution for a specific time (functionalization time) trying to increase the amount of incorporated PTA. After functionalization they were left drying under laboratory atmosphere for 60 s and the used to prepare membrane electrode assemblies.

X-ray Diffraction (XRD) patters were collected using a Pan Analytical Empyrean, powder X-ray diffractometer with a copper anode (Cu Kα radiation, $\lambda = 0.15405$ nm, 30 kV, 30 mA). XRD patterns were recorded over the 2θ angle range from 10° to 90° with a step size of 0.03° and a scan speed of 4°/min.

FT-IR spectra of the samples were examined on a FT-IR spectrometer (Perkin Elmer Spectrum Two).

Scanning Electron Microscopy analysis was performed by using a Philips XL30 ESEM coupled with EDX equipment. Prior to imaging, several pieces of each sample were fixed on the metal stubs with Ag conductive paste.

The composite membranes were sandwiched between two carbon paper electrodes (Toray 40% wet Proofed-E-Tek), covered with a mixture Pt black/C black (30% Pt on Vulcan XC-72, E-Tek) stirred in n-butyl acetate for at least 3 h. A known volume of suspension was left on carbon paper in a Teflon holder until the complete drying of the liquid (at least 24 h). The catalyst loading was 1 mg cm^{-2} of black platinum. The active area was delimited by insulating silicon rubber having an area of 2 cm^2. The Membrane Electrode Assembly (MEA) was then assembled in a single fuel cell apparatus (FuelCellTechnologies, Inc.) and fed with oxygen (99.5% purity), and hydrogen (99.5% purity) humidified at room temperature. Polarization curves were obtained by using a h-tec Fuel Cell Monitor (item 1950) or a Parstat 4000 potentiostat. In the latter case polarization curves were recorded from OCV to 0 V at 100 mV s^{-1}. The current density reported in the following are referred to the apparent active AAM area (2 cm^2).

Electrochemical Impedance Spectroscopy measurements were carried out through a Parstat 4000 potentiostat equipped with an Impedance Analyzer directly connected to the fuel cell. The impedance spectra were recorded in the range 10 kHz–0.1 Hz at 25 °C and an ac amplitude of 10 mV in the activation and ohmic regions. Before each measurement, the fuel cell was stabilized for at least 15 min. The data analysis and equivalent circuit fitting were carried out through a Versa Studio and a ZSimpleWin softwares. Inductive points acquired at high frequencies were removed.

Results and discussion

CS/PTA membrane formation and characterization

Chitosan has been dissolved at different concentration (1–3% w/v) in acetic acid aqueous solution, where it becomes

soluble due to the protonation of the NH_2 groups. CS behaves like a cationic polyelectrolyte and can be ionically cross-linked by anionic species, i.e. $(PW_{12}O_{40})^{3-}$ released by PTA impregnated AAM. In the employed concentrated PTA aqueous solution (0.38 M) only $(PW_{12}O_{40})^{3-}$ anions are present, while lacunary or defective Keggin ions concentration is negligible [21]. When the two electrolytes come in contact, the ionic crosslinking brings to the formation of CS/PTA composite membrane through the following chemical reaction:

$$(PW_{12}O_{40})^{3-} + 3(CS - NH_3^+) \rightarrow (PW_{12}O_{40})^{3-}[CS - NH_3^+]_3 \quad (1)$$

A visual inspection of the prepared membranes proves that they are free-standing, compact, while scanning electron microscopy was employed to study their morphology at the micro-scale and the dependence of their thickness on CS concentration and on reticulation time. In Figs. 1 and 2 we report SEM micrographs relating to the cross section of CS/PTA membranes prepared in different conditions. The images show that the membranes are homogeneous without the formation macrovoid structures (see Figs. 1 and 2), typically observed in polymer film prepared through solution cast processes [22]. This can be attributed to a uniform distribution of cross-links, due to the homogeneous release of PTA^{3-} ions through the pores of the alumina support. The micrographs do not show agglomerates or particles indicating that phase separation between CS and PTA did not occur and contact between PTA and CS was uniform. This implies that the PTA does not re-crystallize, but it electrostatically interacts with CS to form the CS/PTA gel, in agreement with XRD and FTIR results (see below).

In Figs. 1c and 2c we report the estimated thickness as a function of the reticulation time at constant CS concentration and as a function of CS concentration for a constant

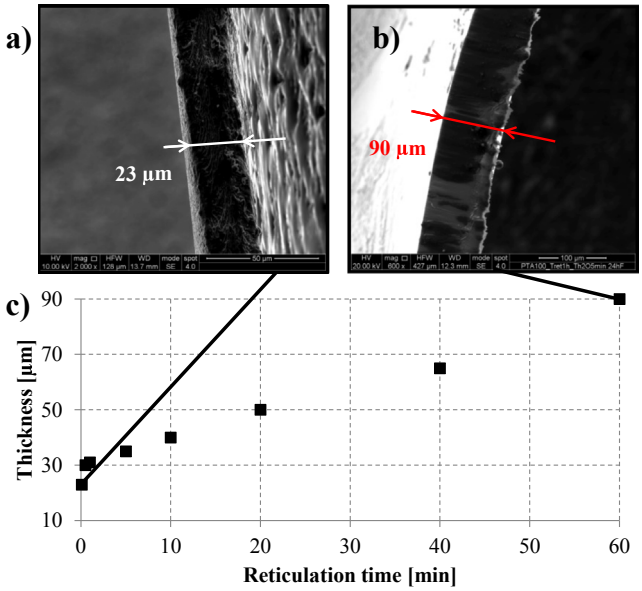

Fig. 1 – SEM cross-section micrographs of CS/PTA membranes prepared with CS concentration 2% w/v, functionalization time 24 h and reticulation time a) 5 s and b) 60 min. Thickness estimated for different reticulation times are reported in c).

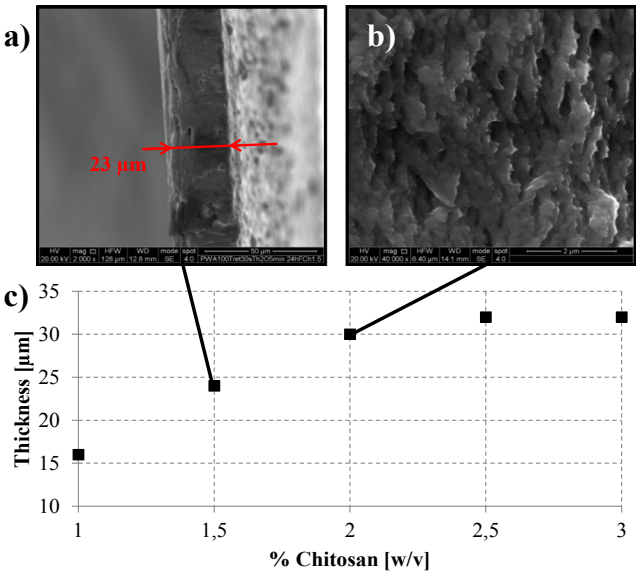

Fig. 2 – SEM micrographs of CS/PTA membranes prepared with reticulation time 30 s, functionalization time 24 h and CS concentration a) 1.5% w/v (cross-section micrograph) and b) 2% w/v (surface micrograph). Thickness estimated for different reticulation times are reported in c).

reticulation time. Each value was estimated averaging the thickness measured in five different points of at least three different samples prepared in the same conditions. The thickness vs. reticulation time plot depicted in Fig. 1c, shows two important features: a fast increasing for low reticulation time (5 s–30 s) and a slower linear increasing for high reticulation time (1 min–60 min). Similarly in Fig. 2c the thickness increases with CS concentration reaching an almost constant value for CS content ≥2.5% w/v when a critical thickness of ~30 µm is reached. It is likely that soon after PTA^{3-} and protonated CS come in contact, they react according to eq. (1) in the aqueous solution. Since we expect that electrostatic interaction between PTA^{3-} and NH_3^+ groups of protonated chitosan is almost instantaneous once they are close enough, it may be postulated that the membrane formation rate is mainly controlled by the diffusion of PTA^{3-} anion through the already formed membrane for thickness >30 µm.

Fig. 3 shows X-ray diffraction patterns relating to CS/PTA membranes synthesized at CS percentages (1%–3%), reticulation time (5 s–60 min) and functionalization time (0 h–24 h). X-ray patterns relating to a) as supplied CS, b) PTA free CS membrane prepared by solution cast [14] and c) PTA powder are also reported to help the peaks identification (Fig. 3a). According to previous results reported in the literature [23,24], six Chitosan polymorphs have been identified: tendon, annealed, '1–2', 'L-2', 'Form I' and 'Form II'. For as supplied CS two peaks having lattice angles 10.6° and 19.8° are present corresponding to the respective equatorial (200) and (020) reflections of the tendon polymorph of chitosan, as already found for CS in the free amino form [25]. Different pattern is recorded for solution cast CS: two sharp peaks at $2\theta = 14°$ and 16.9° are present together with a broad peak roughly centred

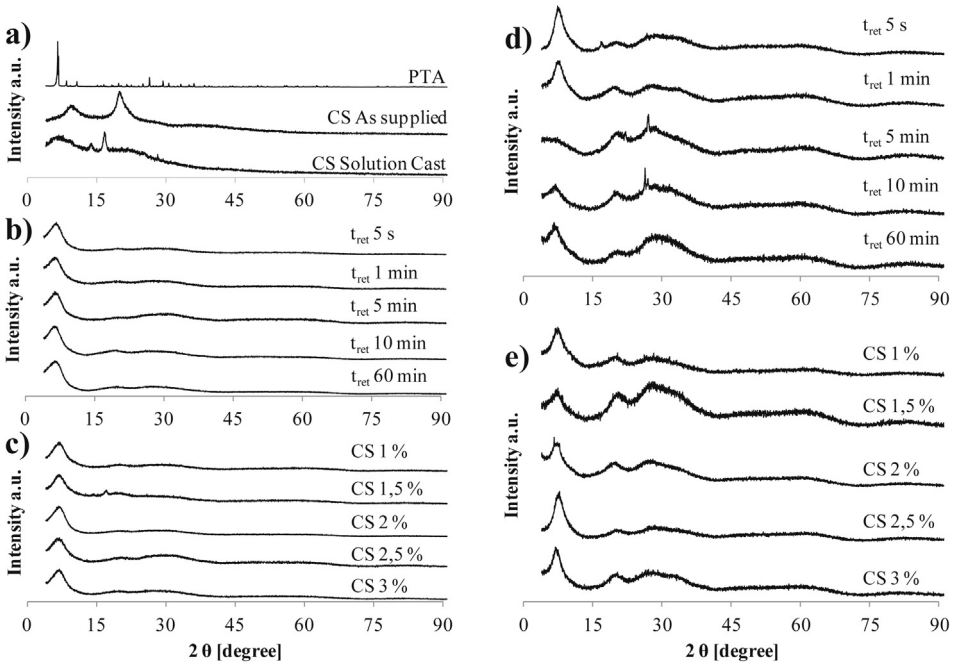

Fig. 3 – X-ray diffraction patterns of: a) as supplied PTA powder, as supplied CS powder and Solution Cast CS; b) CS/PTA membranes prepared with CS concentration 2% w/v as a function of reticulation time; c) CS/PTA membranes prepared with reticulation time 30 s as a function of CS concentration; d) CS/PTA membranes prepared with CS concentration 2% w/v as a function of reticulation time after 24 h of functionalization; e) CS/PTA membranes prepared with reticulation time 30 s as a function of CS concentration after 24 h of functionalization.

at 7.5°. According to the literature [26] such peaks are typical of Form I polymorph with the exception of the peak at reflection angle of 14°, which is reported to be typical of annealed polymorph thus suggesting that mixture of both anhydrous and hydrated crystals is present [27].

The diffraction patterns of CS/PTA membranes (Fig. 3b–e) are different with respect to those recorded with both as supplied CS and solution cast CS membrane: three main peaks at $2\theta = 7.5°$, 20.5° and 28.3° are present, the latter becoming evident after functionalization step. This suggests that Form I polymorph is formed soon after reticulation ($2\theta \sim 7.5$), while functionalization step induces the appearance of Form II polymorph ($2\theta = 20.5°$ and 28.3°). Finally, it is important to stress that no peaks attributed to PTA (see corresponding pattern in Fig. 3a) are present, thus confirming that residual precipitated salt is not present.

The FTIR spectra of CS/PTA films obtained with and without functionalization step prepared with different reticulation times and different CS percentages are reported in Fig. 4.

The spectra of PTA show four characteristic bands (Keggin-type) at around 1080, 983, 891 and 803 cm^{-1} respectively attributed to (P-O), (W-Ot) (Ot refers to the terminal oxygen), (W-Oe-W) (Oe refers to the edge oxygen) and (W-Oc-W) (Oc refers to the corner oxygen) [16,28,29]. The presence of all the characteristic bands of PTA in the CS/PTA complex suggests the preservation of Keggin ions geometry inside the polymer composites.

In the higher wavenumber region all spectra show a peak at 1382 cm^{-1} related to $-CH_3$ symmetric deformation of CS, while the band characteristic of $-NH_2$ bending vibrations (1587 cm^{-1}) is not present. Conversely, the absorption bands characteristic of NH_3^+ bending vibrations appeared at ~1531 cm^{-1} and 1630 cm^{-1} sometimes shifted slightly to lower wavenumber [18]. These results suggest that the $-NH_2$ groups of the chitosan chains in CS/PTA membrane are protonated by acetic acid during the dissolution of CS and by PTA^{3-} during the reticulation step, supporting the presence of ionic bonds between CS and Keggin anions.

As shown in Fig. 4, the broad band starting from 3200 cm^{-1} is assigned to the stretching vibration of N^+-H. This absorption is sensitive to PTA^{3-} ions, because of the strong interaction between the PTA^{3-} ions and NH_3^+ groups by ionic bonding. Such band continued to broaden with increasing reticulation time (Fig. 4a and b), and functionalization time (see Fig. 4e) since more PTA^{3-} ions interacted with the NH_3^+ [30]. A strong broad band appeared at around 3400 cm^{-1} in all spectra of Fig. 4, corresponding to O–H stretching vibrations of the hydroxyl groups of CS.

Thus, we can conclude that almost all the NH_2 groups of chitosan, still present in spite of the reaction with acetic acid, are protonated after reticulation step due to the presence of $H_3PW_{12}O_{40}$, which is strong triprotic acid. It is known that the rigid crystalline structure of pure CS is stabilized mainly by intra- and intermolecular hydrogen bonds [31]. When glucosamine units in CS membranes are protonated, hydrogen bonding involving the NH_2 groups is disrupted, so the rigid crystalline structure weakens. Furthermore, ionic crosslinking, which increases packing of the CS chains, can deform the crystalline regions [32]. This account for the low

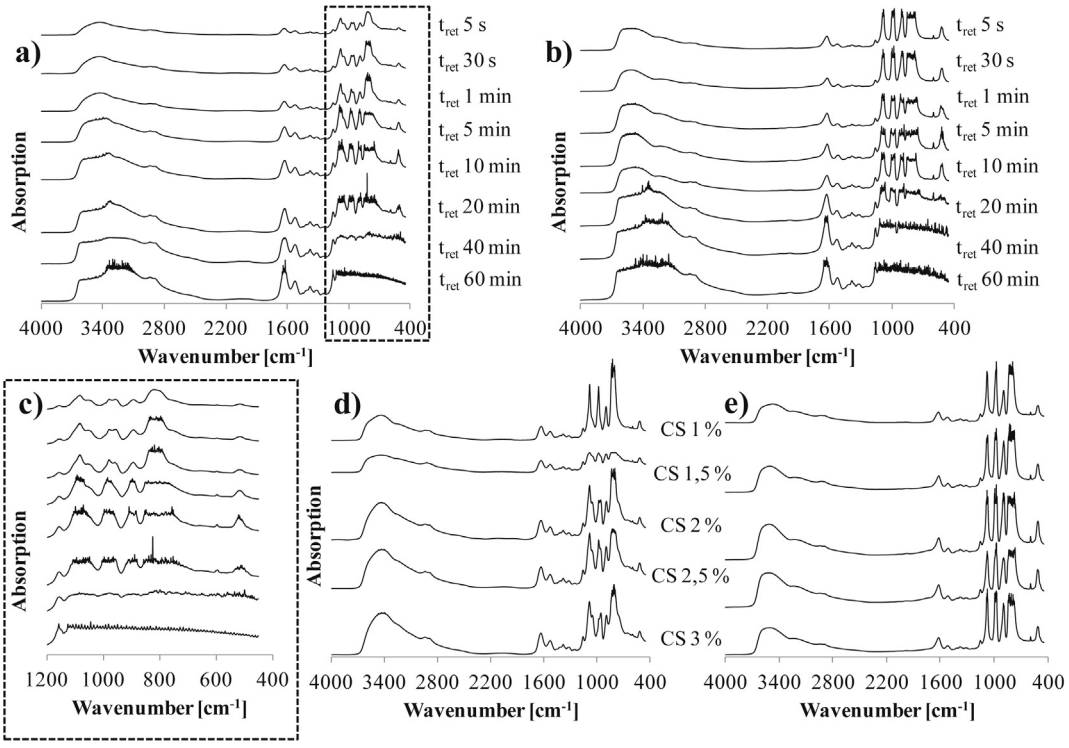

Fig. 4 – FTIR spectra of CS/PTA membranes prepared varying a), b) the reticulation time (CS concentration 2% w/v); d), e) Chitosan percentages (reticulation time 30 s) and functionalization time a), d) 0 h and b), e) 24 h. Magnification of a) is shown in c).

crystallinity of membranes soon after the reticulation step (see Fig. 3b and c). However, according to Fig. 3d and e, membranes become more ordered during the functionalization step, thus suggesting a decrease in the reticulation degree (i.e. in the chains packing) as a consequence of the interaction between the CS/PTA films and the fresh phosphotungstic acidic solution. It is likely that PTA^{3-}, responsible of cross-linking due to interaction with three protonated NH_2 groups, can accept H^+ from fresh $H_3PW_{12}O_{40}$, with consequent reduction of chains packing and presence of H bonded to the Keggin ions and thus available for proton conduction:

$$\left|\left[CS-NH_3^+\right]_3(PW_{12}O_{40})^{3-}\right|_{(CS/PTA)} + |H_3PW_{12}O_{40}|_{(aq)} \downarrow \left|\left[CS-NH_3^+\right]_2(HPW_{12}O_{40})^{2-}\right|_{(CS/PTA)} + \left|\left[CS-NH_3^+\right](H_2PW_{12}O_{40})^{-}\right|_{(CS/PTA)} \quad (2)$$

The occurrence of reaction (2) during the functionalization step explains why membranes' thickness does not change appreciably during immersion in PTA.

Fuel cell performances

The prepared membranes were tested as proton conductors in H_2–O_2 fed room temperature fuel cell. In Fig. 5 we report the OCV as a function of reticulation time and chitosan concentration, after 24 h of functionalization in 0.38 M PTA aqueous solution, recorded under $P_{O2} = P_{H2} = 1$ atm with a Pt loading of 1 mg cm^{-2} at both the electrodes. It is evident that an increase in the reticulation time causes an increase in the measured open circuit voltage, reaching a value of ~1 V for $t_{ret} = 60$ min. This can be explained considering that membranes thickness monotonically increases by increasing reticulation time, according to SEM characterization (see Fig. 1), thus a significant reduction of gas cross over is expected to occur. A slight increase in OCV can also be observed by increasing CS concentration in the preparation solutions at a constant reticulation time (i.e. 30 s, see Fig. 5b). However, even for the highest investigated CS concentration (3% in this work), the measured OCV is lower with respect to those measured for long reticulation time, as expected since not appreciable differences in the membrane thickness were evidenced by SEM increasing the CS concentration from 2.5% to 3% (see Fig. 2).

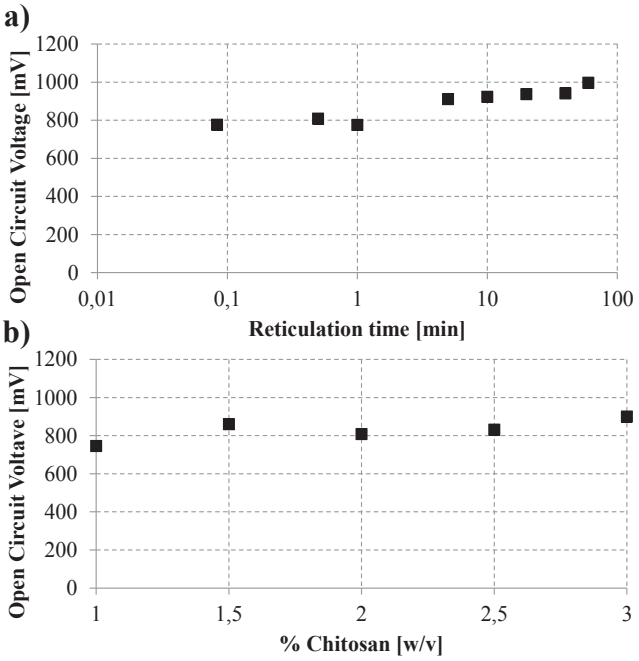

Fig. 5 – OCV measured with MEA prepared using CS/PTA membranes with a) different reticulation times (CS concentration 2% w/v) and b) different CS concentration (reticulation time 30 s), functionalization time 24 h.

Table 1 – Resistance and proton conductivity obtained from slope the ohmic region of the polarization curve vs reticulation time (CS concentration 2% w/v) and Chitosan concentration (reticulation time 30 s), functionalization time 24 h.

t_{ret} [min]	R [mΩ cm^2]	σ [mS cm^{-1}]
5/60	592	3.88
0.5	379	7.91
1	384	8.07
5	539	6.49
10	581	6.88
20	674	7.42
40	741	8.77
60	875	10.4
% CS [w/v]	R [mΩ cm^2]	σ [mS cm^{-1}]
1	424	3.77
1.5	376	6.38
2	379	7.92
2.5	416	7.69
3	505	6.34

In Fig. 6 we compare the polarization curves recorded during fuel cell operation with CS/PTA membranes prepared at constant CS concentration (2% w/v) as a function of reticulation time (see also SI). It is interesting to mention that for reticulation time up to 20 min, three different regions are clearly distinguishable: 1) the activation region close to the OCV where charge transfer is the rate determining step; 2) the ohmic region, where the main losses are due to membrane resistance; 3) mass transport region, where mass transfer controls the overall reaction rate. The latter disappears for longer reticulation time, i.e. when the membrane thickness is so high that a significant contribution of the electromotive force is dissipated in ohmic losses hindering current to reach the diffusion limited regime. This is in agreement with the slopes of the ohmic regions reported in Table 1 as a function of the reticulation time, which are found to increase for $t_{ret} \geq 30$ s. From the resistance, R_m, it is possible to estimate the conductivity of the membrane, σ, according o the following relationship:

$$\sigma = L/R_m\, A \qquad (3)$$

where L is the membrane thickness and A the geometric area of the membrane. σ resulted to be dependent on the reticulation time, thus suggesting that the reticulation time influences not only the membrane thickness but also its capacity of proton transfer.

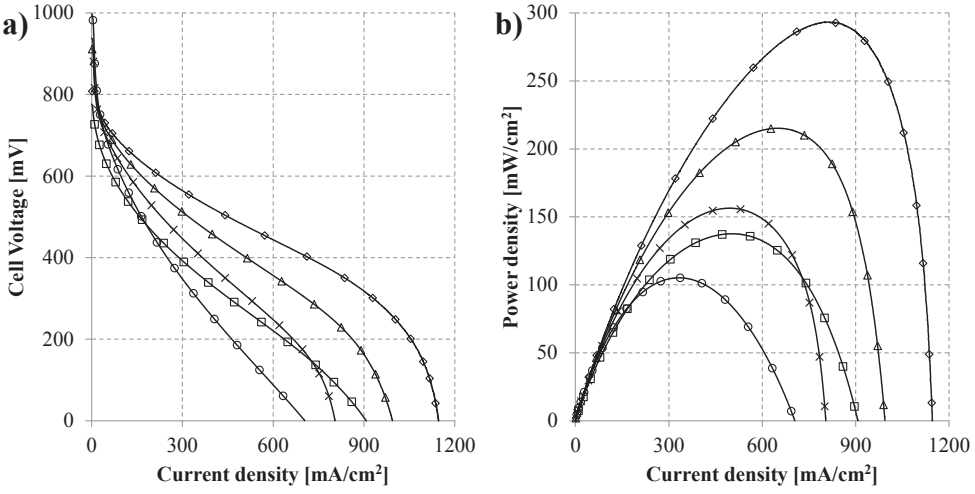

Fig. 6 – a) Polarization curves and b) power density curves for CS/PTA membranes prepared at CS concentration 2% w/v, functionalization time 24 h and different reticulation times: (□) 5 s, (◊) 30 s, (Δ) 5 min, (×) 20 min and (○) 60 min.

Concerning the membranes obtained for very short reticulation time (i.e. 5 s), their poor performance is mainly attributed to very low OCV value, which in turn can be related to the formation of a more porous membrane. This can also explain the low conductivity of such membranes if compared to the values estimated for thicker CS/PTA films (see Table 1). According to [33], where a detailed investigation on the effect of Nafion membrane thickness on the proton conductivity is reported, measured proton conductivity decreases for thin membranes and attributed this effect to discontinuities in structure between the surface and ''bulk'' regions of the membrane, which are more important for thin membranes where the ratio of surface to ''bulk'' pores is greater. The value of Table 1 suggests that σ strongly increases when reticulation time goes from 5 s to 30 s due the corresponding increasing in membrane thickness and a reduction in contact resistances. Concerning the effect of CS concentration such phenomenon can explain the increase in proton conductivity with increasing CS % up to 2 w/v. For higher CS concentration it seems that this effect is cancelled by the formation of a more compact membrane in spite of the almost coincident thickness.

The power density vs current curves corresponding to the V–I curves of Fig. 6a are shown in Fig. 6b. It is evident that the highest peak power, i.e. ~300 mW cm^{-2}, is measured with the membrane reticulated for 30 s, while it decreases by increasing reticulation time (see SI). Moreover for CS/PTA membrane prepared with CS concentration of 2% w/v and reticulation time of 30 s, an increase in the gas pressure (P_{H2} = P_{O2} = 1.2 atm) and in Pt load at the cathode side (1.5 mg cm^{-2}) allowed to obtain a better performance as shown in Fig. 7 with peak power up to 410 mW cm^{-2}.

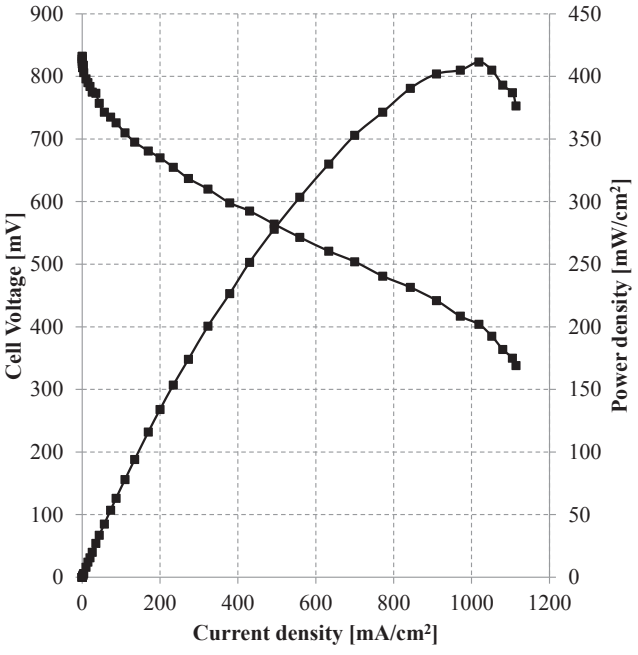

Fig. 7 – Best Fuel Cell performance's polarization curve of CS/PTA membranes prepared with CS concentration 2% w/v, reticulation time 30 s and functionalization time 24 h. MEA was prepared with Pt load 1.5 mg cm^{-2} cathode side and 1 mg cm^{-2} anode side. Both the hydrogen and the oxygen were fed at 1.2 bar.

Membrane functionalization time effect

In Fig. 8 we compare the fuel cell polarization curves recorded with membranes synthesised with a reticulation time of 30 s and a CS concentration of 2% w/v as a function of the functionalization time, i.e. immersion in 0.38 M PTA solution (0, 12, 24 and 48 h). It is clearly evident that if functionalization steps in not performed (i.e. 0 h) the membrane performance is very poor with a polarization curve dominated by the ohmic control and a low peak power of 32 mW cm^{-2}. A significant improvement is obtained after 12 h and 24 h of immersion in 0.38 M PTA, while further increase in functionalization reduces the performance probably due to an excessive reduction in the chains packing according to Eq. (2). SEM characterization of the membranes cross sections showed that the thickness is not significantly influenced by functionalization time, thus for membranes of Fig. 8 it is ~30 μm allowing estimating the conductivity according to Eq. (3) (see SI). Immersion in PTA aqueous solution for 24 h allows measuring σ of 14 times higher with respect to the conductivity of the as prepared membranes. This confirms that during functionalization reaction (see Eq. (2)) proton conductivity of membranes increases.

Proton conductivity of pure CS at 25 °C is reported to be $4 \cdot 10^{-5}$ S cm^{-1} and $3.5 \cdot 10^{-3}$ S cm^{-1} for films coagulated in NaOH [34] and prepared by solution-cast [30], respectively. According to the literature [35] proton conductivity of PTA powder at 25 °C is in between $2.0 \cdot 10^{-2}$ and $7.2 \cdot 10^{-2}$ S cm^{-1}. The values measured in this work suggest that a significant contribution to membranes' proton conductivity derives from PTA.

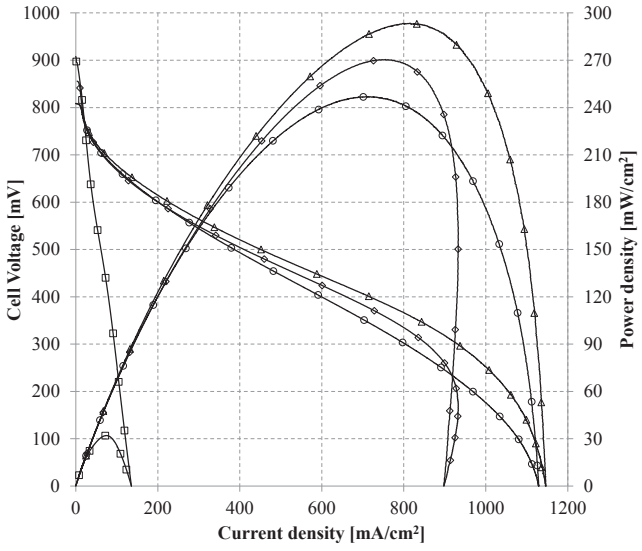

Fig. 8 – Polarization curves of CS/PTA membranes prepared with CS concentration 2% w/v, reticulation time 30 s and functionalization time (□) 0 h, (◊) 12 h, (Δ) 24 h, and (○) 48 h.

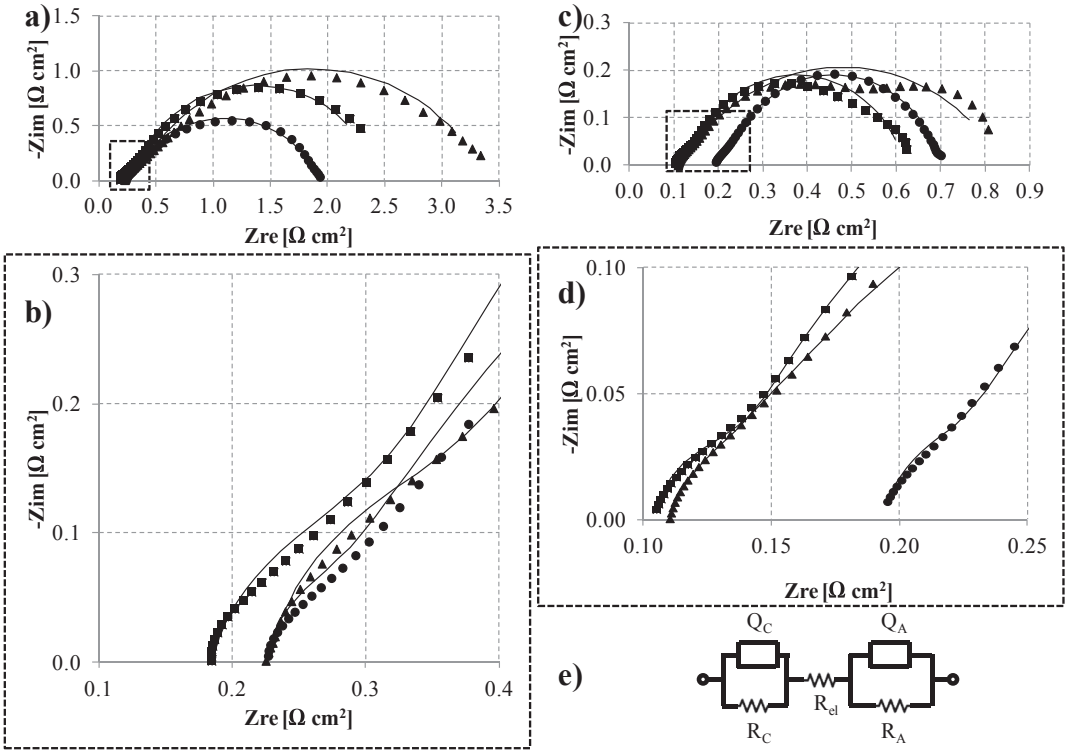

Fig. 9 – Nyquist plots for CS/PTA membranes prepared with a CS concentration of 2% w/v, reticulation time of 30 s and functionalization time of (▲) 12 h, (■) 24 h and (●) 48 h. The spectra are recorded a), b) in the activation region and c), d) in the ohmic region. All spectra are fitted, see continuous line (–), through the equivalent circuit shown in e).

In situ-EIS studies

Information on the electrode kinetic and the membrane resistance was collected through in-situ ac impedance measurements carried out in the fuel cell fed with H_2/O_2 at 25 °C gas and cell temperature. In Fig. 9 we report the Nyquist plots recorded in the activation (U_E = 700 mV) and ohmic (U_E = 450 mV) regions of the polarization curve for a MEA with CS/PTA membranes prepared starting from a 2% w/v CS solution with t_{ret} = 30 s and functionalization time of 12, 24 and 48 h. The spectra were interpreted according to a simple equivalent circuit (Fig. 9e), where the membrane resistance (R_{el}), i.e. the real axis intercept at the highest frequency, is in series with two parallels relating to the two electrode reacting interfaces. Both the anode and the cathode are simulated by a constant phase element (Q_A and Q_C respectively) in parallel to a charge-transfer resistance (R_A and R_C respectively). This model is generally accepted for H_2/O_2 fuel cell systems at low and moderate current densities [36–39] and fits well most of EIS spectra of this work. The contact resistances are assumed negligible as verified by measuring the ohmic resistance of the cell components.

The fitting parameters are reported in Table 2. A careful inspection of the parameters clearly shows that anode works

Table 2 – Fitting parameters estimated from EIS spectra recorded in the activation and ohmic region for CS/PTA membranes prepared with a CS concentration of 2% w/v, reticulation time 30 s and functionalization time of 0 h, 12 h, 24 h and 48 h.

t funz [h]	R_{el} [Ω cm^2]	R_A [Ω cm^2]	Q_A [S · sec^n · cm^{-2}]	n_A	R_C [Ω cm^2]	Q_C [S · sec^n · cm^{-2}]	n_C	σ [mS cm^{-1}]	χ^2
Activation region									
0	450	76.5	4 10^{-6}	0.875	1209	0.000145	0.663	0.00667	1.85 10^{-3}
12	0.226	0.1	0.0103	0.978	3.06	0.0605	0.749	13.2	3.31 10^{-3}
24	0.213	0.0924	0.0106	0.98	1.30	0.0669	0.851	14.1	1.36 10^{-3}
48	0.231	0.0867	0.0209	1	1.52	0.0781	0.9	12.9	5.99 10^{-3}
Ohmic region									
0	530	78.4	6.57 10^{-7}	1	423	0.000119	0.625	0.00566	1.68 10^{-3}
12	0.109	0.0993	0.0578	1	0.722	0.259	0.661	27.5	2.41 10^{-3}
24	0.105	0.0313	0.0265	0.973	0.482	0.142	0.848	28.6	2.35 10^{-3}
48	0.193	0.0321	0.0468	0.919	0.473	0.129	0.861	15.5	5.07 10^{-3}

as almost ideally non polarisable interface with charge transfer resistance very close to zero, in agreement with the behaviour expected for hydrogen oxidation on platinum. Slightly higher values were estimated for R_C, i.e. for O_2 reduction in agreement with the sluggish kinetic of this reaction. The R_C values of Table 2 are higher with respect to those estimated with MEAs prepared in the same conditions but at the open circuit voltage [20]. Such reduction is a consequence of the higher overvoltage for spectra of Fig. 9. If we assume that dependence of current on electrode potential is expressed by Butler–Volmer equation, i.e. if we assume charge transfer as the rate determining step at the cathode, R_C results to be inversely proportional to the circulating current according to the following relationship:

$$i = i_0 \exp(-\alpha n F\eta/RT) \quad (4)$$

obtaining Eq. (5):

$$R_C = |\partial\eta/\partial i| = RT/(\alpha n F i) \quad (5)$$

where R is the ideal gas constant, T is the absolute temperature, α is transfer coefficient, $n = 2$ [40] is the electrons amount transferred during the rate determining step, F is the Faraday constant and i is the current density. Through the Eq. (5), the R_C are ~0.06 and 1 Ω cm^2 when calculated in the ohmic region and in the activation region, respectively, thus showing a good agreement with the values recorded through the EIS spectra.

The CS/PTA membrane resistance R_{el} recorded in the activation region is higher than the ones recorded in the ohmic region. For a dry cell, which works in the activation region, whole spectra are shifted toward the positive side of the real axis. These results were interpreted in term of increase of ohmic resistance in dry condition and increase of the polarisation and diffusion resistances in flooding condition, when the fuel cell works in the ohmic region [39].

Impedance Spectroscopy was also employed to study the electrical behaviour of the MEAs as a function of the membrane fabrication conditions. More specifically we have investigated the dependence of EIS spectra recorded in the activation and ohmic regions of polarization curves for MEA prepared with CS/PTA membranes as a function of the reticulation time and CS concentration (see SI). In Fig. 10a and b we report the estimated R_{el} values in MEAs prepared with CS/PTA membranes prepared starting from a 2% w/v CS solution vs reticulation time and in Fig. 10b R_{el} estimated for membranes prepared at constant reticulation time (30 s) as a function of CS concentration.

Increasing the CS concentration and the reticulation time respectively, in the ohmic region recorded values of R_{el} increased by 0.089–0.29 and by 0.1–0.28 Ω cm^2, while in the activation region R_{el} increased by 0.18–0.37 Ω cm^{-2} and by 0.17–0.77 Ω cm^2.

Fuel cell performance stability and durability

At the present no data are reported in the literature about durability and performance stability of fuel cell H_2–O_2 fed working with chitosan – based electrolyte. It is obvious that essential requirement for a fuel cell electrolyte is the good chemical and mechanical stability in the fuel cell

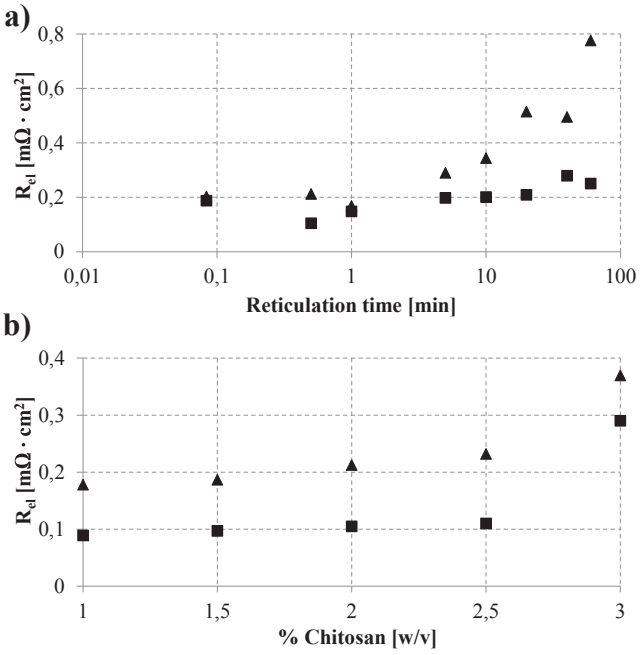

Fig. 10 – Estimated R_{el} values in MEAs prepared with CS/PTA membranes recorded (▲) in the activation region and (■) in the ohmic region plotted a) vs. reticulation (CS 2% w/v) and b) vs. CS concentration (reticulation time 30 s), functionalization time 24 h.

environment. Previous results obtained with AAM/PTA fuel cell [11] show a strong degradation of the performance due to the dissolution of both the acidic pore-filler and the alumina membrane in the water produced at the cathode/electrolyte interface. The performance loss decreases for CS/PTA filled AAM and disappears for solution cast CS/PTA film electrolyte which produces a constant 10 mW cm^{-2} power output for at least 10 h, as reported in our previous work [14]. At variance with the cross-linking process on preformed solution cast CS film, the ionotropic gelation process shown in this work allows to obtain higher power output (up to 410 mW cm^{-2}) attributed to an uniform ionic bond distribution due to the in-situ cross-linking of NH_3^+ groups of CS with PTA^{3-} anions.

The stability of the performance was studied by recording successive polarization curves, as reported in Fig. 11a. It can be observed a progressive improvement of the performance up to the 8th cycle due to the hydration of the membrane and electrode/electrolyte interface. Afterwards the polarization curve is stable. The power output vs. time of the 2% w/v CS concentration and 30 s reticulation time CS/PTA fuel cell under a constant cell voltage of 0.45 V is reported in Fig. 11b and c. After a steep decreasing during the first 10–20 min, the power density reaches a constant for a few hours. From Fig. 11c it can be also detected a good dynamic stability of the cell, which is able to restart after 12 h off, even if at lower power density. Also during restart the early minutes of polarization are detrimental with a rapid drop of performance.

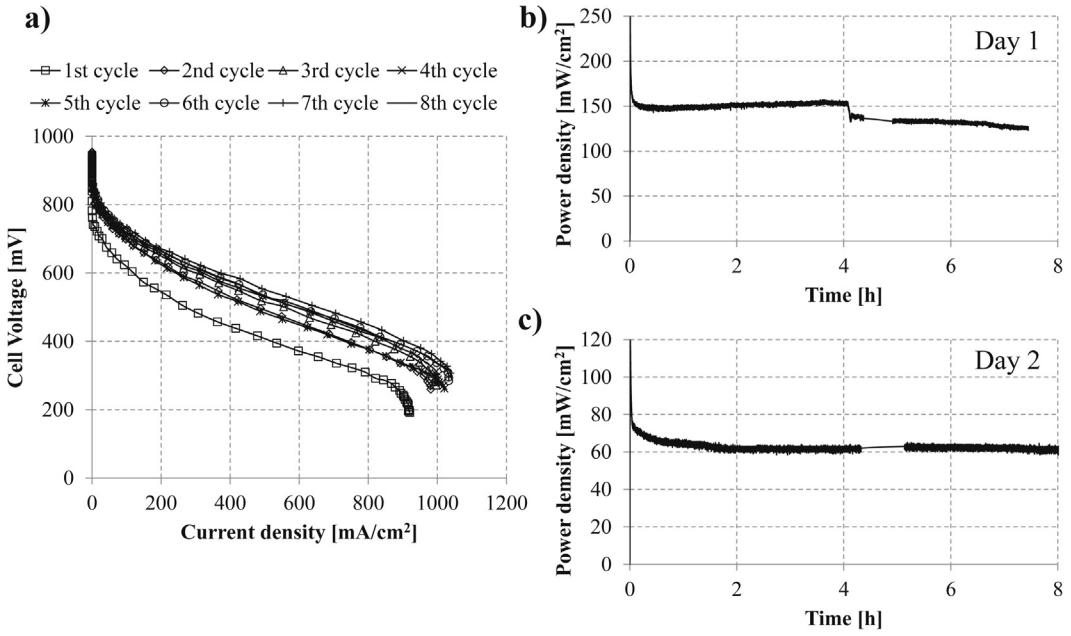

Fig. 11 – a) Successive polarization curves and b) power output vs. time (Ue = 450 mV) recorded for a CS/PTA membrane prepared with 2% w/v CS concentration, reticulation time 30 s and functionalization time 24 h. The power output vs. time restarted after 12 h powered off is shown in c).

Summary and conclusions

Chitosan-phosphotungstic membranes have been prepared by ionotropic gelation of CS using anodic alumina membrane as porous medium and phosphotungstate anions as ionic crosslinkers. The films were synthesised varying the reticulation time, the CS concentration and functionalization time. They resulted to be free standing and compact independently on the investigated fabrication conditions. The morphological characterization, performed by SEM, allowed to evidence the formation of homogeneous membranes, whose thickness resulted to be strongly influenced by reticulation time, and slightly dependent on CS concentration in the starting solution.

X-ray and FTIR confirmed that membrane show very poor crystallinity soon after reticulation, and that crystallinity is enhanced by the functionalization step, i.e. by immersion in a phosphotungstic acid aqueous solution.

The prepared membranes were employed as proton conductors in H_2–O_2 low temperature fuel cell. Their performances resulted to be strongly influence by reticulation time, CS concentration and, more importantly, by functionalization, which resulted to be essential for H^+ conduction. Optimization of the fabrication conditions allowed to get a peak power of 300 mW cm^{-2}, while the optimization of the electrode reaction kinetic allowed to increase the peak power to 410 mW cm^{-2}.

Stability test showed that power density decreases significantly in the first 10–20 min, while it is almost constant for 2–3 h. In spite of a good dynamic stability of the cell, which is able to restart after 12 h off, the early minutes of polarization are detrimental with a further reduction of the stationary power density. The increase of long term stability is the main issue for a possible application of CS membranes in H_2–O_2 membranes.

Acknowledgements

Italian MiUR is acknowledged for funding through PON R&C 2007–2013 ("TESEO"- PON02_00153-2939517).

Appendix A. Supplementary data

Supplementary data related to this article can be found at http://dx.doi.org/10.1016/j.ijhydene.2015.06.083.

REFERENCES

[1] Beuscher U, Cleghorn SJC, Johnson WB. Challenges for PEM fuel cell membranes. Int J Energ Res 2005;29:1103–12.
[2] Barbir F, Yazici S. Status and development of PEM fuel cell technology. Int J Energ Res 2008;32:369–78.
[3] Ratlamwala TAH, El-Sinawi AH, Gadalla MA, Aidan A. Performance analysis of a new designed PEM fuel cell. Int J Energ Res 2012;36:1121–32.
[4] Wan Y, Creber KAM, Peppley B, Bui VT. Chitosan-based solid electrolyte composite membranes I. Preparation and characterization. J Memb Sci 2006;280:666–74.
[5] Rinaudo M. Chitin and chitosan: properties and applications. Prog Polym Sci 2006;31:603–32.
[6] Ma J, Sahai Y. Chitosan biopolymer for fuel cell applications. Carbohyd Polym 2013;92:955–75.
[7] Zhao CJ, Lin HD, Cui ZM, Li XF, Na H, Xing W. Highly conductive, methanol resistant fuel cell membranes

fabricated by layer-by-layer self-assembly of inorganic heteropolyacid. J Power Sources 2009;194:168–74.
[8] Cui ZM, Xing W, Liu CP, Liao JH, Zhang H. Chitosan/heteropolyacid composite membranes for direct methanol fuel cell. J Power Sources 2009;188:24–9.
[9] Mohanapriya S, Bhat SD, Sahu AK, Pitchumani S, Sridhar P, Shukla AK. A new mixed-matrix membrane for DMFCs. Energ Environ Sci 2009;2:1210–6.
[10] Shakeri SE, Ghaffarian SR, Tohidian M, Bahlakeh G, Taranejoo S. Polyelectrolyte nanocomposite membranes, based on Chitosan-phosphotungstic acid complex and Montmorillonite for fuel cells applications. J Macromol Sci B 2013;52:1226–41.
[11] Bocchetta P, Conciauro F, Di Quarto F. Nanoscale membrane electrode assemblies based on porous anodic alumina for hydrogen-oxygen fuel cell. J Solid State Electr 2007;11:1253–61.
[12] Bocchetta P, Ferraro R, Di Quarto F. Advances in anodic alumina membranes thin film fuel cell: CsH2PO4 pore-filler as proton conductor at room temperature. J Power Sources 2009;187:49–56.
[13] Bocchetta P, Conciauro F, Santamaria M, Di Quarto F. Cs-0.86(NH4)(1.14)SO4Te(OH)(6) in porous anodic alumina for micro fuel cell applications. Electrochim Acta 2011;56:3845–51.
[14] Bocchetta P, Conciauro F, Santamaria M, Di Quarto F. Fuel cell performances of bio-membranes made of Chitosan-polyelectrolyte thin films and nanowires into anodic alumina membranes. ECS Trans 2012;41:79–89.
[15] Ma J, Choudhury NA, Sahai Y, Buchheit RG. A high performance direct borohydride fuel cell employing cross-linked chitosan membrane. J Power Sources 2011;196:8257–64.
[16] Cui ZM, Liu CP, Lu TH, Xing W. Polyelectrolyte complexes of chitosan and phosphotungstic acid as proton-conducting membranes for direct methanol fuel cells. J Power Sources 2007;167:94–9.
[17] Tohidian M, Ghaffarian SR, Shakeri SE, Dashtimoghadam E, Hasani-Sadrabadi MM. Organically modified montmorillonite and chitosan-phosphotungstic acid complex nanocomposites as high performance membranes for fuel cell applications. J Solid State Electr 2013;17:2123–37.
[18] Choudhury NA, Ma J, Sahai Y. High performance and eco-friendly chitosan hydrogel membrane electrolytes for direct borohydride fuel cells. J Power Sources 2012;210:358–65.
[19] Majid SR, Arof AK. Conductivity studies and performance of chitosan based polymer electrolytes in H-2/air fuel cell. Polym Advan Technol 2009;20:524–8.
[20] Santamaria M, Pecoraro CM, Di Quarto F, Bocchetta P. Chitosan–phosphotungstic acid complex as membranes for low temperature H_2–O_2 fuel cell. J Power Sources 2015;276:189–94.
[21] Zhu ZR, Tain R, Rhodes C. A study of the decomposition behaviour of 12-tungstophosphate heteropolyacid in solution. Can J Chem 2003;81:1044–50.
[22] Kaiser V, Stropnik C, Musil V, Brumen M. Morphology of solidified polysulfone structures obtained by wet phase separation. Eur Polym J 2007;43:2515–24.
[23] Zhang W, Zhang J, Jiang Q, Xia W. Physicochemical and structural characteristics of chitosan nanopowders prepared by ultrafine milling. Carbohyd Polym 2012;87:309–13.
[24] Cervera MF, Heinamaki J, Rasanen M, Maunu SL, Karjalainen M, Acosta OMN, et al. Solid-state characterization of chitosans derived from lobster chitin. Carbohyd Polym 2004;58:401–8.
[25] Saito H, Tabeta R, Ogawa K. High-resolution solid-state C-13 Nmr-study of cChitosan and its salts with acids – conformational characterization of polymorphs and Helical structures as viewed from the conformation-dependent C-13 chemical-shifts. Macromolecules 1987;20:2424–30.
[26] Samuels RJ. Solid state characterization of the structure of chitosan films. J Polym Sci Polym Phys Ed 1981;19:1081–105.
[27] Belamie E, Domard A, GiraudGuille MM. Study of the solid-state hydrolysis of chitosan in presence of HCl. J Polym Sci Pol Chem 1997;35:3181–91.
[28] Rocchiccioli-Deltcheff C, Fournier M, Franck R, Thouvenot R. Vibrational investigations of polyoxometalates. 2. Evidence for anion-anion interactions in molybdenum(VI) and tungsten(VI) compounds related to the Keggin structure. Inorg Chem 1983;22:207–16.
[29] Aparicio M, Mosa J, Etienne A, Duran A. Proton-conducting methacrylate-silica sol-gel membranes containing tungstophosphoric acid. J Power Sources 2005;145:231–6.
[30] Cui Z, Xiang Y, Si JJ, Yang M, Zhang Q, Zhang T. Ionic interactions between sulfuric acid and chitosan membranes. Carbohyd Polym 2008;73:111–6.
[31] Wan Y, Creber KAM, Peppley B, Tam Bui V. Ionic conductivity and tensile properties of hydroxyethyl and hydroxypropyl chitosan membranes. J Polym Sci Part B: Polym Phys 2004;42:1379–97.
[32] Lee ST, Mi FL, Shen YJ, Shyu SS. Equilibrium and kinetic studies of copper(II) ion uptake by chitosan-tripolyphosphate chelating resin. Polymer 2001;42:1879–92.
[33] Slade S, Campbell SA, Ralph TR, Walsh FC. Ionic conductivity of an extruded Nafion 1100 EW series of membranes. J Electrochem Soc 2002;149:A1556–64.
[34] Ramirez-Salgado J. Study of basic biopolymer as proton membrane for fuel cell systems. Electrochim Acta 2007;52:3766–78.
[35] Nakamura O, Ogino I. Electrical conductivities of some hydrates of dodecamolybdophosphoric acid and dodecatungstophosphoric acid and their mixed crystals. Mater Res Bull 1982;17:231–4.
[36] Wagner N, Schnurnberger W, Muller B, Lang M. Electrochemical impedance spectra of solid-oxide fuel cells and polymer membrane fuel cells. Electrochim Acta 1998;43:3785–93.
[37] Wagner N. Characterization of membrane electrode assemblies in polymer electrolyte fuel cells using a.c. impedance spectroscopy. J Appl Electrochem 2002;32:859–63.
[38] Makharia R, Mathias MF, Baker DR. Measurement of catalyst layer electrolyte resistance in PEFCs using electrochemical impedance spectroscopy. J Electrochem Soc 2005;152:A970–7.
[39] Tant S, Rosini S, Thivel PX, Druart F, Rakotondrainibe A, Geneston T, et al. An algorithm for diagnosis of proton exchange membrane fuel cells by electrochemical impedance spectroscopy. Electrochim Acta 2014;135:368–79.
[40] Mainka J, Maranzana G, Dillet J, Didierjean S, Lottin O. On the estimation of high frequency parameters of proton exchange membrane fuel cells via electrochemical impedance spectroscopy. J Power Sources 2014;253:381–91.